Journal of Drug Targeting

ISSN: 1061-186X (Print) 1029-2330 (Online) Journal homepage: https://www.tandfonline.com/loi/idrt20

Anti-inflammatory flurbiprofen nasal powders for nose-to-brain delivery in Alzheimer's disease

Laura Tiozzo Fasiolo, Michele Dario Manniello, Fabrizio Bortolotti, Francesca Buttini, Alessandra Rossi, Fabio Sonvico, Paolo Colombo, Georgia Valsami, Gaia Colombo & Paola Russo

To cite this article: Laura Tiozzo Fasiolo, Michele Dario Manniello, Fabrizio Bortolotti, Francesca Buttini, Alessandra Rossi, Fabio Sonvico, Paolo Colombo, Georgia Valsami, Gaia Colombo & Paola Russo (2019): Anti-inflammatory flurbiprofen nasal powders for nose-to-brain delivery in Alzheimer's disease, Journal of Drug Targeting, DOI: 10.1080/1061186X.2019.1574300

To link to this article: https://doi.org/10.1080/1061186X.2019.1574300

Accepted author version posted online: 29 Jan 2019.

Original paper

Anti-inflammatory flurbiprofen nasal powders for nose-to-brain delivery in Alzheimer's disease

Laura Tiozzo Fasiolo[a,b], Michele Dario Manniello[c], Fabrizio Bortolotti[b], Francesca Buttini[a], Alessandra Rossi[a], Fabio Sonvico[a], Paolo Colombo[a,d], Georgia Valsami[e], Gaia Colombo[b*] and Paola Russo[c**]

[a]*Department of Food and Drug, University of Parma, Parma, Italy*
[b]*Department of Life Sciences and Biotechnology, University of Ferrara, Ferrara, Italy*
[c]*Department of Pharmacy, University of Salerno, Fisciano (SA), Italy*
[d]*PlumeStars Srl, Parma, Italy*
[e]*Department of Pharmacy, National and Kapodistrian University of Athens, Athens, Greece*

*Corresponding Author:
Gaia Colombo, PhD.
Department of Life Sciences and Biotechnology
University of Ferrara
Via Fossato di Mortara 17/19
44121 Ferrara, Italy
Tel: +39 0532 455909
E-mail: clmgai@unife.it
http://orcid.org/0000-0001-9033-2305

**Corresponding Author:
Paola Russo, PhD.
Department of Pharmacy
University of Salerno
Via Giovanni Paolo II 132
84084 Fisciano (SA), Italy
Tel: +39 089 969256
E-mail: paorusso@unisa.it
http://orcid.org/0000-0002-4362-4388

Abstract

Neuroinflammation occurs in the early stages of Alzheimer's disease (AD). Thus, anti-inflammatory drugs in this asymptomatic initial phase could slow down AD progression, provided they enter the brain. Direct nose-to-brain drug transport occurs along olfactory or trigeminal nerves, bypassing the blood-brain barrier. Nasal administration may enable the drug to access the brain.

Here, flurbiprofen powders for nose-to-brain drug transport in early AD-related neuroinflammation were studied. Their target product profile contemplates drug powder deposition in the nasal cavity, prompt dissolution in the mucosal fluid and attainment of saturation concentration to maximise diffusion in the tissue. Aiming to increase drug disposition into brain, poorly soluble flurbiprofen requires the construction of nasal powder microparticles actively deposited in nose for prompt drug release.

Two groups of powders were formulated, composed of flurbiprofen acid or flurbiprofen sodium salt. Two spray dryer apparatuses, differing for spray and drying mechanisms and particle collection, were applied to impact on the characteristics of the microparticulate powders. Flurbiprofen sodium nasal powders disclosed prompt dissolution and fast *ex vivo* transport across rabbit nasal mucosa, superior to the acid form, in particular when the powder was prepared using the Nano B-90 spray dryer at the lowest drying air temperature.

Keywords

Flurbiprofen; Alzheimer’s disease; nasal powder; nose-to-brain; microparticle; particle engineering

1. Introduction

Alzheimer's Disease (AD) is an age-related multifactorial neurodegeneration, characterised by a progressive reduction of cognitive performance and memory loss. It is the most common form of dementia, presently affecting over 46 million individuals worldwide. The number is estimated to increase dramatically by 2050 [1,2]. Few drugs are approved so far, which mainly act on some of the AD clinical signs.

The advancements in the comprehension of AD pathogenesis urge that treatments begin before the appearance of neurological and cognitive decline. It is also recognised that a multi-target approach with drugs in combination may be necessary, which also includes an anti-inflammatory component [3,4] and insulin [5].

In fact, based on the evidence that the deposition of beta amyloid (Aβ) fragments in AD brain induces a marked neuro-inflammatory response, researchers hypothesised that neuroinflammation could be a therapeutic target [6]. The hypothesis was reasonable also in light of observational studies on patients with rheumatoid arthritis, evidencing the association between long-term exposure to non-steroidal anti-inflammatory drugs (NSAIDs) and delayed AD onset [7]. However, clinical trials in which different NSAIDs (e.g. ibuprofen, celecoxib, *R*-flurbiprofen, aspirin, etc.) were administered to symptomatic AD patients [8,9], showed a substantial lack of efficacy in subjects that were already cognitively impaired.

One current opinion about these failures is that the late inflammation in the central nervous system (CNS) of AD patients may have a beneficial 'protective' function as the disease progresses. Nevertheless, new hopes raise from more recent animal studies, reporting that inflammation in the CNS begins much earlier and likely before the formation of amyloid plaques [10]. This early inflammation was seen in studies with transgenic animal models, as human markers have not yet been identified. Provided it can be detected in asymptomatic individuals, early inflammation could become the target of an NSAID-based therapy. Several reports show that the conventional cyclooxygenase-inhibition mechanism of action of NSAIDs could be effective before the clinical signs appear [4,11].

Among the NSAIDs tested, tarenflurbil or *R*-flurbiprofen had been selected in clinical trials on AD patients as modulator of γ-secretase rather than as anti-inflammatory agent. The modulation of this enzyme reduced $A\beta_{42}$ accumulation *in vitro* and *in vivo* (transgenic AD model mouse) [12-14]. The *R*-enantiomer of flurbiprofen has no anti-cyclooxygenase activity [15]. However, in a phase III clinical trial, oral administration of tarenflurbil failed to produce a clinical benefit on mild to moderate AD patients. Weak pharmacological activity and poor pharmacokinetics were advocated as reasons of the failure [16,17].

It is recognised that NSAIDs have low disposition in the CNS by systemic circulation [18]. If flurbiprofen reached the brain at pharmacodynamically relevant concentrations, it could play a role in fighting the neuroinflammation associated with the early events of AD pathogenesis. Nasal administration may enable a more effective access to the CNS when drugs poorly cross the blood brain barrier (BBB). In fact, direct nose-to-brain drug transport can occur along the olfactory or trigeminal pathways, bypassing the BBB [19]. In addition, nasal delivery can reduce the systemic exposure to the drug and first-pass metabolism compared to oral administration [20,21].

We have recently reviewed the nasal powders as dosage forms, underlining indisputable advantages compared to liquids from the biopharmaceutical and stability perspectives [22]. In particular, powders enhance the transport of the drug across the nasal barrier. After prompt drug dissolution in the fluid lining the nasal mucosa, a saturation concentration sustains the diffusion gradient across the tissue [23,24]. This is the target product profile for powder deposition in the nasal cavity when the CNS is the drug target site [25,26]. A nasal powder formulation of flurbiprofen aiming to increase the drug disposition into the brain [15] requires the construction of microparticles to be actively or passively deposited into the nose for a prompt drug release. Therefore, the aim of this research was to study flurbiprofen nasal powder formulations effective for nasal deposition and drug transport to brain through nasal mucosa. Flurbiprofen microparticles useful for nasal powder delivery were constructed. Using a powder technology typical for the manufacturing of microparticles for inhalation, the flurbiprofen API was transformed into micronized particles by spray drying [27]. By employing the drug in acid form or its sodium salt, microparticles were prepared with or without excipients, using two lab scale spray drying equipment and different operating conditions. The obtained nasal powders were characterised *in vitro*, and the *ex vivo* drug transport was assessed. The final nasal product construction and *in vivo* evaluation will be described in a subsequent paper.

2. Materials and methods

2.1 Materials

Flurbiprofen raw material or API (batch n° T17121044) was kindly donated by Recordati S.p.A. (I-Milano). This drug substance was used for the preparation of the HPLC analytical standards and also as reference powder in the *in vitro* and *ex vivo* transport experiments. Mannitol (Ph. Eur.) was supplied by Lisapharma S.p.A. (I-Erba) and lecithin (Lipoid® S45) by Lipoid AG (CH-Steinhausen). HPLC-grade acetonitrile and isopropyl alcohol were supplied by Sigma-Aldrich® (St. Louis, MO, USA). All other reagents and solvents were analytical grade.

2.2 Methods

2.2.1 Flurbiprofen HPLC assay

Flurbiprofen quantification was carried out by reversed-phase high performance liquid chromatography (HPLC) with UV-Vis detection (Agilent 1100 series, Santa Clara, CA, USA). Isocratic elution was carried out with a NaH_2PO_4 20 mM:CH_3CN (40:60) mobile phase (pH 3.0 ± 0.1) at room temperature. The detection wavelength was set at 244 nm. The stationary phase was a Zorbax Eclipse XDB column (C18, 5 µm, 4.6 x 15 mm; Agilent, Santa Clara, CA, USA). The flow rate was 0.8 ml/min. The injection volume was 20 µl (auto-sampler). In these conditions, the retention time of flurbiprofen was 4.6 min.

The method was developed in-house and validated with respect to linearity range (concentration range 0.13 - 4.2 µl/ml, $y=112.6x - 0.1506$, $R^2=1$; n=3), repeatability (0.089% RSD for peak area, n=6 injections) and limit of quantification (6.2 ng/ml).

The analytical standard solution was prepared from a 200 µg/ml stock solution of flurbiprofen API dissolved in methanol. This stock solution was prepared and stored at 2-8 °C for up to one month. On each day of analysis an aliquot of stock solution was diluted with the mobile phase to a final drug concentration of about 4 µg/ml, which was within the method's linearity range.

2.2.2 Manufacturing of flurbiprofen spray-dried microparticles

Spray drying was carried out using both the Mini B-191 and the Nano B-90 spray dryers (BÜCHI Labortechnik, CH-Flawil). Micronized powders of flurbiprofen (FB-COOH) or its sodium salt (FB-COONa) were prepared by spray drying the drug, alone or together with lecithin (ratio 92:8 w/w, respectively), keeping the total solid concentration in the liquid feed

at 2% (w/v) in all cases. For FB-COOH microparticles, the liquid feed (100 ml) was a hydro-alcoholic suspension of FB-COOH (water/isopropanol 70:30 v/v). FB-COOH was first dissolved in the alcohol, then this solution was added to water precipitating the drug particles. For the sodium salt microparticles, FB-COOH was dispersed in water (2% w/v), then NaOH 1M was added until the drug was completely dissolved (final pH 7.4), according to Manniello et al. [28].

Finally, for the production of FB-COOH microparticles with lecithin, the phospholipid was solubilised in isopropanol together with flurbiprofen, then the solution was added to water. To produce FB-COONa/lecithin microparticles, lecithin was dissolved in isopropanol and this solution added to the FB-COONa aqueous solution. In this case, the water/isopropanol ratio was 95:5 (v/v).

<Table 1 near here>

Table 1 summarises the apparatus, the liquid feed composition and the drying temperatures. 100 ml of each liquid feed were processed by the Mini B-191 spray dryer in the following operating conditions: drying air flow 500 L/min, aspiration rate 100%, air pressure 6 atm, liquid feed flow 5 ml/min, inlet temperature 90 or 120 °C, nozzle diameter 0.7 mm. With the Nano B-90 equipment, the operating conditions were the following: drying air flow 100 L/min, liquid feed flow 1.5 ml/min, relative spray rate 100%, inlet temperature 40 or 70 °C, spray cap 7.0 µm.

2.2.3 Physico-chemical characterisation of flurbiprofen spray-dried microparticles

Drug content

Drug content was determined by HPLC after dissolving an accurately weighed amount of powder (5 mg) in methanol or phosphate buffered saline pH 7.4 (PBS; KCl 0.2 g/l; NaCl 8 g/l; Na_2HPO_4 1.15 g/l; KH_2PO_4 0.2 g/l), depending on whether the powder contained FB-COOH or FB-COONa. The obtained solutions were diluted with mobile phase before injection. Measurements were performed in triplicate for each batch.

Morphology

The morphology of raw material and spray-dried microparticles was evaluated by scanning electron microscopy (SEM). Sample preparation and operating conditions are reported elsewhere [29]. A Carl Zeiss EVO MA 10 microscope was used with a secondary electron

detector (Carl Zeiss SMT Ltd., Cambridge, UK) equipped with a LEICA EMSCD005 metallizer to deposit a 200–400 Å thick gold layer. Analyses were conducted at 17 keV.

Particle size analysis

The size distribution was determined for flurbiprofen API and the various spray-dried microparticles by laser light diffraction with an apparatus equipped with a 45 mm focal lens (Mastersizer X, Malvern Instruments Ltd, Worcestershire, UK). The FB-COOH raw material and spray-dried microparticles were suspended in water, whereas FB-COONa microparticles were suspended in dichloromethane at a concentration of 0.9 mg/ml. Each suspension was sonicated for 5 min for homogeneous particle dispersion. Then, the suspension was diluted dropwise in 100 ml of the same vehicle until proper obscuration was reached. Size data are expressed as $d_{v,10}$, $d_{v,50}$ and $d_{v,90}$ (n=3 samples *per* batch). The SPAN value was calculated according to Equation 1:

$$Span = \frac{[d_{v,90} - d_{v,10}]}{d_{v,50}} \qquad \text{(Eq. 1)}$$

Thermal analysis

Differential Scanning Calorimetry (DSC) analysis was carried out on the flurbiprofen raw material and drug microparticles (DSC 822e, Mettler Toledo, Columbus, OH, USA). 11.0 ± 0.5 mg of sample were weighed in a 40 µl aluminium pan (MTS Mettler Toledo microbalance, Columbus, OH, USA), sealed and pinholed. Samples were heated up to 350 °C at a scanning rate of 10 °C/min in a single cycle of measurement [30].

For FB-COONa microparticles, preliminary dehydration was carried out to remove water, heating the samples up to 130 °C at a scanning rate of 10 °C/min and leaving them at 130 °C for 15 min. Then, the pan was cooled down at room temperature and heated again as above reported.

X-ray diffraction analysis

X-ray diffraction (PXRD) of flurbiprofen raw material and microparticles was carried out on a BRUKER AXS D8 Advance diffractometer (Bruker, Billerica, MA, USA), equipped with a curved graphite crystal, using Cu Kα radiation (λ = 1.5406 Å). The scanning rate was 2θ/θ; $3° \leq 2\theta \leq 50°$; Step 0.02°; Step time 2 s.

2.2.4 Biopharmaceutical characterisation of flurbiprofen spray-dried microparticles

In vitro flurbiprofen dissolution/transport across an artificial membrane

Vertical Franz-type diffusion cells with 0.58 cm^2 diffusion area (Vetrotecnica, I-Padova) were used to estimate *in vitro* the dissolution of flurbiprofen microparticles [31]. A regenerated cellulose membrane (MW cut-off 12,000–14,000 Da, Dexstar Visking, Medicell International Ltd, London, UK) separated the donor and receptor compartments. The receptor compartment was filled with 5 ml of PBS pH 7.4. The donor compartment was loaded with 5 mg of powder, independently of the drug content. Then, 100 µl of PBS pH 7.4 was added. The cells were kept in a water bath at 37 °C during the experiment. At pre-determined time points up to 4h, 100 µl samples of receptor solution were withdrawn for analysis and replaced by an equal volume of fresh PBS. Experiments were performed in triplicate.

At the end a drug mass balance >90% was assessed (sum of the amounts of flurbiprofen recovered from receptor, donor and membrane).

The steady-state flux (J_{SS}) of flurbiprofen across the membrane was calculated from the slope of the linear part of the curve obtained by plotting the mass transported per unit area against time [32].

Ex vivo flurbiprofen transport across rabbit nasal mucosa

The *ex vivo* transport of flurbiprofen across excised rabbit nasal mucosa was studied with the same Franz-type cells used for the *in vitro* dissolution experiments (0.58 cm^2). The nasal mucosa was peeled off the nasal septum of rabbits, extracted within 2 h from the animal's death from the heads supplied by a local slaughterhouse (Pola S.r.l., Finale Emilia, Italy). The extraction procedure is described elsewhere [24]. The diffusion cells were assembled with the tissue's mucosal side facing the donor compartment. The receptor compartment was filled with 5 ml of PBS pH 7.4. The assembled cells were equilibrated for 10 min at 37 °C before introducing the formulation. As for the *in vitro* dissolution studies, about 5 mg of FB-COOH microparticles or FB-COONa microparticles and 100 µl of PBS pH 7.4 were loaded. Flurbiprofen API and a saturated solution in PBS pH 7.4 (1.5 mg/ml, 0.5 ml) were tested for comparison purposes. The saturated solution was prepared by adding an excess amount of flurbiprofen API to PBS pH 7.4 and letting the suspension under magnetic stirring at 37 °C for 24 h. Then, the supernatant was separated by centrifugation (8,000 rpm, 5 min) and used as donor formulation.

Experiments lasted 4 h [33]. The receptor medium was sampled at the beginning of the experiment and then every hour, and replaced with fresh medium. At the end of the

experiment the residual drug in the donor compartment was quantitatively recovered by rinsing with PBS. Drug accumulated within the tissue thickness was extracted by cutting the mucosa with a surgical blade and homogenizing it in 5 ml of water with Ultra-Turrax® IKA homogenizer (T10 basic model, IKA® Werke GmbH & Co. KG, D-Staufen) for 3 minutes. Two millilitres of methanol were then added and homogenisation continued for further 30 seconds to disrupt the cell membranes and complete the extraction. The homogenates were centrifuged (10,000 rpm, 10 min) and the obtained supernatant was diluted with mobile phase for injection. The mass balance was calculated as seen. The minimum number of replicates was 5.

The steady-state flux of flurbiprofen across the mucosa was calculated as seen.

2.2.5 Statistical analysis

Data were compared by applying an unpaired two-tailed Student's t-test. $P < 0.05$ was considered to indicate statistical significance.

3. Results and Discussion

Focusing on nasal powders, formulations suitable for the nose-to-brain delivery of flurbiprofen need to reach effective drug concentration at the site of deposition. This objective requires that the solid formulation deposits and dissolves quickly on the wet nasal mucosa, reaching high and persistent drug concentration on the absorption site.

Flurbiprofen raw material (API) available in this research was unsuitable as powder for nasal administration, mainly due to the very low solubility in water (8 mg/L at 22 °C) [34] and to powder micromeritics. In general, for nasal powder formulations the residence time on the mucosa is short (though longer for powders than for liquids). Therefore, the drug dissolution rate in the nasal aqueous fluids should be as high as possible to promptly provide the maximal drug concentration at absorption site. The equilibrium solubility of flurbiprofen API in deionized water and in PBS pH 7.4 at 37 °C was experimentally determined, resulting equal to 0.029 ± 0.004 g/L and 1.5 ± 0.1 g/L, respectively. Flurbiprofen is a weak carboxylic acid with pH-dependent solubility, justifying the higher value at pH 7.4. Thus, the presence of the carboxylic moiety was exploited to obtain a sodium salt and to improve the drug aqueous solubility, while particle size reduction via spray drying was exploited to increase the dissolution rate.

3.1 Spray-dried flurbiprofen microparticles manufacturing: yield, particle size, morphology and drug content

Spray drying is a widely employed technique for constructing microparticles for inhalation, by drying a liquid feed solution or suspension in a continuous and efficient process [22,35,36]. Flurbiprofen micronized powders were manufactured by spray drying the drug either as acid form suspension (FB-COOH) or as sodium salt solution (FB-COONa). In one series of preparations, spray-dried microparticles were formulated by adding 8% (w/w) of soybean lecithin. The intention was to modify the drug particle surface by providing adhesion properties, also favouring a subsequent agglomeration step functional for nasal deposition of these powders [24,37].

Two spray dryer apparatuses were used, differing in spray generation, drying air flow and temperature, and particle collection, namely the Mini B-191 and the Nano B-90 (BÜCHI). The aim was to study the equipment's impact on the size and shape and biopharmaceutical properties of the dried microparticles. In particular, the Nano B-90 apparatus exploits a newer technology for laboratory scale production, operating at lower temperature and requiring minimal volumes of liquid feed to obtain micronized powders with high yields [38-40].

As shown in Table 1, the composition of the liquid feed was not the same for all microparticles, depending on whether the drug was spray-dried as acid or sodium salt form. For the acid drug, a hydro-alcoholic feed suspension was employed, obtained by dissolving the drug in isopropanol and precipitating it with water. The flurbiprofen sodium feed solution was obtained by dissolving the API in water with stoichiometric NaOH until a limpid solution was formed (pH 7.4).

<Table 2 near here>

Using the Mini B-191 equipment, the yield of the spray-dried product did not exceed 40% and it was even lower when preparing FB-COONa microparticles (Table 2). Several unsuccessful attempts were made to increase this low yield, basically by modifying the liquid feed, i.e., doubling of the total solid concentration (4% w/v), increasing the percent of organic solvent when spraying FB-COOH or adding 10-20% (v/v) of isopropanol when spraying FB-COONa. In all cases, the critical step was the droplet evaporation, with massive adhesion of material to the drying chamber wall.

The same liquid feeds used on the Mini B-191 were processed with the Nano B-90 spray dryer. This apparatus is equipped with an electrostatic particle collector where, differently from conventional spray drying cyclones, particle separation should be independent of particle mass. The Nano B-90 spray dryer did not allow to obtain microparticles of flurbiprofen acid. This was due to the fact that the liquid droplets are generated by a piezoelectric system, vibrating a perforated membrane, which can only process solutions or very diluted suspensions. Indeed, the FB-COOH liquid feeds were concentrated suspensions. In contrast, the drying process with Nano B-90 was quite efficient with the FB-COONa solutions and yields were significantly improved compared to the Mini B-191, even when the inlet temperature was 40 °C (Table 2). The low evaporation temperature could be an advantage of the Nano B-90 for thermal stability of sensitive drugs, even though the drying phase is prolonged.

When lecithin was included in the microparticle composition (8% w/w), barely no powder was obtained from spray drying it with FB-COOH on the Mini B-191: the liquid feed droplets stuck to the evaporation chamber glass wall and did not give rise to powders. With FB-COONa, the lecithin presence required the organic solvent (isopropanol) in the liquid feed. A very small amount of powder was obtained with lecithin and the drug salt on the Mini B-191. Similarly to what happened with the drug alone, the use of the Nano B-90 spray dryer

increased the yield of FB-COONa also in presence of lecithin. At 70 °C, using 5% (v/v) isopropanol as organic solvent, the yield was about 46%. The isopropanol percentage in the feed was increased from 5% to 8% (v/v) aiming to work at lower inlet temperature (40 °C), without substantial improvements of the yield (data not shown). However, the use of ethanol as alternative organic solvent, maximized the powder yield (data not shown) [41].

<Figure 1 near here>

SEM micrographs of spray-dried powders are shown in Figure 1. Using the Mini B-191 spray dryer, the morphology of FB-COOH microparticles (Fig. 1, F2) did not change substantially compared to the raw material (Fig. 1, API); the spray drying slightly reduced the size narrowing the particle size distribution (Table 2). In this case, flurbiprofen had been dissolved in isopropanol and precipitated with water due to an antisolvent effect, with the formation of a new particle population. In contrast, the spray drying of flurbiprofen sodium water solution led to a mix of small spherical and corrugated large particles (Fig. 1, F3). These particles had a significantly lower $d_{v,50}$ ($P < 0.05$) than F2 and their size distribution displaced towards small values. Their shape and collapsed morphology derived from the complete dissolution of flurbiprofen sodium in the liquid feed and were a sign of hollow particles. In spray drying, the microparticle structure is governed by the ratio between solvent evaporation rate and solute diffusion rate, as described by the Peclet number. In dependence of the respective prevalence of the two rates, a number higher or lower than 1.0 explains the formation of hollow or solid particles [42]. During drying of the FB-COONa solution droplets using the Mini B-191, the drug diffusion rate was slower than the solvent evaporation rate due to the high air temperature. This provided a sufficient drug enrichment of the droplet surface for the formation of hollow particles, as evidenced by the presence of collapsed structures [43]. Using the Nano B-90 equipment, the particles were smaller than their counterpart obtained with the Mini B-191. The size difference between F3 and F13_70 or F13_40 formulations was significant at $P < 0.05$ for the $d_{v,50}$ value. The lower particle size reached with the Nano B-90 could be due to the lower inlet temperatures that decreased the rate of solvent evaporation during droplet drying [44]. Here, in the comparison between the two spray dryers processing the flurbiprofen sodium aqueous solution, the feed composition was the same (i.e., same diffusion rate in the droplet), but the inlet temperature was lower with the Nano B-90 spray dryer (i.e., different droplet evaporation rate). This was one of the factors contributing to the formation of smaller flurbiprofen sodium microparticles. Another operating parameter

influencing the particle size is the rate at which the feed is sprayed. This was lower for the Nano B-90 spray dryer *versus* the MiniB-191 and contributed to the size reduction of the particles, as observed by Belotti et al. [35]. Finally, the procedure of particle collection of the Nano B-90 may have influenced the microparticle size distribution, as the equipment retained the particles regardless of their size.

Furthermore, when the inlet temperature of the Nano B-90 was reduced from 70° to 40 °C, the average diameter ($d_{v,50}$) of the resulting microparticles further decreased from 5.69 ± 0.36 µm to 4.31 ± 0.44 ($P < 0.05$). The size difference between F13_70 and F13_40 paired with a different appearance of the particles at SEM (Fig. 1, F13_70 and F13_40). The F13_40 smaller microparticles were spherical and smoother and very few appeared corrugated or collapsed compared to F13_70. Such morphology was interpreted again by the Peclet number: if the droplet evaporation rate is lower than the diffusion rate, the Peclet number is less than 1.0 and smaller solid particles will form by slowing down the surface drug enrichment during drying and delaying the drug precipitation.

The Nano B-90 microparticles of FB-COONa with lecithin (F15_70) were less spherical with a slightly rough surface (Fig. 1, F15_70) compared to those without the phospholipid. They were coated by lecithin [45,46] and partially aggregated because lecithin acted as an agglomerating agent. Laser light scattering analysis confirmed that these particles were 4-fold as bigger as without lecithin (Table 2). This result has not to be considered negative since the nasal administration does not have the same small size restriction of pulmonary microparticles. Non-respirable particles are more suitable for nasal administration since they avoid the lung deposition.

Flurbiprofen content in the spray-dried microparticles is reported in Table 2. Flurbiprofen in F2 was around 100%, whereas it was not for the salt powders. Drug content analysis indicated that FB-COONa always precipitated in dihydrate form, explaining the 81% of flurbiprofen in F3 (Table 2). Dihydrate formation occurs often with sodium salts of various drugs [47] and the salt corresponds to the formula described in the US Pharmacopoeia monograph of flurbiprofen sodium, where the drug water content ranges between 11.3-12.5%. In FB-COONa microparticles the flurbiprofen content slightly decreased from the Mini B-191 to the Nano B-90. This was attributed to some residual adsorbed water caused by the lower evaporation temperatures used with the Nano B-90. These data indicated that flurbiprofen was stable during spray drying, even at the high temperatures of the Mini B-191 spray dryer.

3.2 Microparticle solid state characteristics

Thermal analysis by differential scanning calorimetry (DSC) compared flurbiprofen raw material with the spray-dried microparticles to assess the effect of the process on the drug solid state.

<Figure 2 near here>

The raw material (Fig. 2, trace D) showed an endothermal event at 122 °C, which corresponded to flurbiprofen melting. The Ph. Eur. flurbiprofen monograph reports a melting point of 114-116 °C. The same endothermic peak was seen for the Mini B-191 FB-COOH microparticles (F2; Fig. 2, trace E). This confirmed that spray drying of flurbiprofen acid did not modify the solid state of the original substance.

A study by David et al. [48] evaluated the effect of the counterion on the solid state properties of a series flurbiprofen salts with different amines. They observed that the relationship between salt formation and melting point is not unidirectional, i.e., the salt can melt at lower or higher temperature than the parent drug depending on the counterion, which determines the ionic and intermolecular forces within the solid particle. In addition, the hydration water molecules could be involved as they bring additional H-bonding capacity into the solid structure.

The DSC traces of the sodium salt microparticles show a relevant thermal event around 100 °C due to the loss of the two water molecules (thermogram not shown). Figure 2 shows all the thermograms relative to microparticles and flurbiprofen API. In order to avoid an overlapping in the figure between the water peak and the thermal event of flurbiprofen melting, the samples underwent a dehydration treatment prior to DSC scan. De-hydration removed the bound water as well as any residual water from the spray drying. Then, the endothermic peak at about 240 °C with the Nano B-90 FB-COONa microparticles (F13_70; Fig. 2, trace A) and the disappearance of the fusion peak of flurbiprofen at 122 °C indicated the sodium salt presence.

The thermogram of Mini B-191 FB-COONa microparticles (F3; Fig. 2, trace B) showed two thermal events that could be related to the existence of a second polymorph: the first event characterised by the endothermic peak around 160 °C, should correspond to the melting of a metastable polymorphic form of FB-COONa. The subsequent exothermic event around 200 °C preceded the fusion of the more stable polymorph around 240 °C [49]. As drying and solid particle formation are fast with the Mini B-191 due to the high inlet temperature, the

formation of a metastable polymorph is possible [50].
The temperatures and energies associated with these transitions are summarised in Table 3.

<Table 3 near here>

The Nano B-90 microparticles containing lecithin displayed the same two endothermic peaks, with no effect on the thermal behaviour of flurbiprofen sodium due to the presence of lecithin (data not shown).
Although spray drying often leads to amorphous powders [51], in this study, independently on the apparatus employed, all spray-dried microparticles were crystalline, as shown by the sharp peaks in the X-ray diffraction spectra. In particular, the FB-COOH microparticles (F2) retained the crystalline phase of the raw material (Fig. 3, top). However, the intensity of the signal was lower for the spray-dried microparticles. This indicates that the F2 crystals were smaller than the raw material ones. In X-ray diffraction, the bigger the crystal's size, the higher the number of diffracted electrons, i.e., the signal's intensity. The crystal's size is determined by the crystallization process: if the process is fast, the crystals have little time to grow. Indeed, spray drying had reduced the size of F2 compared to the raw material (Table 2).

<Figure 3 near here>

The X-ray diffractograms of the flurbiprofen sodium salt showed a different crystal phase compared to the acid. The Mini B-191 (F3) and the Nano B-90 flurbiprofen sodium microparticles dried at 70 °C (F13_70) showed superimposable diffractograms, with the exception of the sharp peak at 7°-8° 2θ that corresponded to a minimal residue of flurbiprofen acid (Fig. 3, centre). The crystal phase of the salt remained the same independently of the spray dryer, whereas the peak intensities did not. The less intense F3 peaks again depended on the crystals' size. However, in this case the respective intensities did not match with the measured particle size because F3 was bigger than F13_70 (Table 2). We considered that with the two spray dryers the size distribution of the microparticles depends not only on solvent evaporation, but also on the mechanism of particle collection. Thus, a relationship between size and X-ray diffraction intensity is not straightforward.
F13_40 microparticles showed differences compared to F13_70 (Fig. 3, bottom). The new peak at 5° 2θ, the shift of the two peaks between 31°-34° 2θ and the shift of the peak at 46°

2θ, indicated the presence of a second polymorph. The height ratio of the peak at 5° 2θ and that at 3° 2θ indicated that this polymorph accounted for about 20% of the powder. In addition, the diffraction between 5° and 16° 2θ was attributed to the presence of some amorph flurbiprofen. Overall, F13_40 was less crystalline than F13_70 and this was related to the evaporation temperature.

The presence of lecithin in the composition of the Nano B-90 flurbiprofen sodium microparticles did not modify the X-ray diffraction pattern, except for the intensity, which was higher for the lecithin-containing microparticles (data not shown).

3.3 Biopharmaceutical characteristics of flurbiprofen spray-dried microparticles

3.3.1 Flurbiprofen dissolution/transport across a non-partitioning membrane

The test apparatus was a Franz cell with a non-partitioning membrane of regenerated cellulose separating the donor from the receptor. In these conditions the drug transport across the membrane from the microparticles was governed by the dissolution of the solid formulation deposited on the membrane. In other words, given that the membrane had the same permeability for all the powders, the transport profiles across were determined by the drug concentration in the donor, resulting from the dissolution rate of the microparticles on the membrane. Flurbiprofen dissolution/transport was measured over 4 hours, being aware that this time frame exceeded the residence time of prompt release formulations in the nasal cavity [52].

Flurbiprofen is very slightly soluble in water and this hinders its dissolution. The spray drying process of the FB-COOH powder did not significantly reduce the particle size, compared to the raw material. Then, spray drying was not effective for increasing the flurbiprofen dissolution rate in PBS pH 7.4 (Fig. 4). In addition, the solubility in the buffer pH 7.4 at 37 °C was 1.5 mg/ml, unchanged compared to the raw material.

The powders of flurbiprofen sodium salt (FB-COONa) were prepared by spray drying an aqueous solution of flurbiprofen obtained by titration with sodium hydroxide. Regardless of the equipment and process conditions used for their manufacturing, the dissolution/transport of all the FB-COONa microparticles was prompt, faster than for the acid form and not significantly different among the powders prepared (Fig. 4). After 4 h, the amount of flurbiprofen released per unit area of membrane for formulations F3 (Mini B-191), F13_70 and F13_40 (Nano B-90 microparticles spray-dried at 70 °C and 40 °C) and F15_70 with lecithin were 6.19 ± 0.02 mg cm^{-2}, 6.02 ± 0.11 mg cm^{-2}, 6.23 ± 0.29 mg cm^{-2} and 5.89 ± 0.13

mg cm^{-2}, respectively. The linearity of the release profiles during the first hour indicated the presence of a constant gradient across the cellulose membrane, allowing for the calculation of the initial drug flux from the straight line slope (Table 4).

<Figure 4 near here>

Compared to flurbiprofen, the 10-fold higher solubility of the salt in the release medium significantly increased the flux ($P < 0.05$) of FB-COONa microparticles, without substantial variations deriving from the spray drying conditions. This implied that the sodium flurbiprofen powders dissolved at a similar rate independently of the differences observed in their particle size distributions. In the experimental set-up with the Franz cell, powder dissolution occurred on a non-partitioning membrane and was controlled by drug solubility, membrane transport and concentration in the receptor medium [53]. Thus, the particle size distributions were not enough different for affecting the dissolution rate of the very soluble FB-COONa microparticles on the membrane. The lecithin presence in FB-COONa microparticle composition (F15_70) did not modify the drug dissolution transport rate.
In the present test conditions, the salt microparticles led to the dissolution and transport of more than 80% of the loaded flurbiprofen at the end of the 4 hours. The flux significantly slowed down beyond 90 minutes, reasonably due to the reduction of drug concentration in the donor and its increase in the receptor. Indeed, the fraction dissolved in 1 hour (>40% of the loaded drug) and the measured fluxes (Table 4) were regarded as a relevant property for the purpose of nose-to-brain delivery.

<Table 4 near here>

3.3.2 Ex vivo flurbiprofen transport across rabbit nasal mucosa

Flurbiprofen belongs to the Class II of the Biopharmaceutical Classification System of drugs, i.e., it has low aqueous solubility and high permeability. Aiming to its administration in powder form via the nasal route, the target product profile implies the capability to promptly dissolve in the nasal fluid, partitioning in the mucosa and diffuse across it. Thus, the transport of flurbiprofen across excised rabbit nasal mucosa from the spray-dried microparticles was studied taking as references the flurbiprofen API and its saturated solution in PBS pH 7.4. These two permeation profiles, together with all the profiles of the prepared powders, are reproduced in Figure 5. From the API saturated solution, the drug permeated across the tissue

at 4 h was 0.60 ± 0.03 mg per unit area. This amount corresponded to about 47% of the flurbiprofen introduced in the donor. With the liquid formulation, the solubility in the aqueous medium limited the amount loaded in donor compartment. This dose limitation endorsed the interest toward the use of a powder as nasal dosage form. Indeed, using the flurbiprofen API in powder form, the drug transport was improved (1.02 ± 0.11 mg cm^{-2} at 4 h), even though the difference with the saturated solution profile became statistically significant only after 2 h ($P < 0.05$). The linearity of the API powder profile up to 2h suggested that steady state conditions could be envisaged. It is reasonable to foresee that the dissolution of drug powder maintained saturated the small fluid volume layering on the mucosa. Thus, the concentration gradient could remain quasi constant across the barrier. Then, the steady state flux through the membrane was calculated, assuming that during the two hours the concentration of flurbiprofen in the donor was equal to the solubility.

<Figure 5 near here>

The calculated steady state flux (J_{SS}) with the solid API was higher than the value presented by the saturated solution (Table 4). In fact, the initial flurbiprofen concentration in the saturated solution progressively decreased in consequence of the drug transport. This result amplified the relevance of a solid dosage form of flurbiprofen for nose-to-brain absorption. Then, flurbiprofen acid was processed by spray drying to obtain a micronized powder (F2). This flurbiprofen spray-dried powder (Fig. 5) increased the drug transported across the mucosa membrane *versus* the raw material (1.95 ± 0.09 mg cm^{-2} in 4h, corresponding to 23 ± 3% of 5 mg flurbiprofen loaded; $P < 0.05$). The amount of flurbiprofen accumulated in the rabbit nasal mucosa was 0.13 ± 0.01 mg vs 0.09 ± 0.01 mg for the API and F2 microparticles, respectively.

The drug transport from the two powders across the mucosa marginally paired with the *in vitro* dissolution/transport across the artificial membrane. In the latter case, the flux from F2 microparticles was higher but not significantly different from the raw material ($P = 0.44$) (see Fig. 4, Table 4). The regenerated cellulose membrane and the excised nasal mucosa are different barriers, the latter being thicker, with permeability depending on the distribution coefficient of the diffusing molecule. One would expect that, from the same formulation, flurbiprofen transport occurred more slowly across the mucosa than the artificial membrane. This was not the case for F2. The actual powder distribution on the mucosa of F2 spray-dried microparticles compared to the cellulose membrane, may have impacted the effective surface

for microparticle dissolution (Table 4). The biological barrier combined positively with F2 microparticle characteristics relevant to transport, like wettability and dissolution, not disregarding the deposition and contact between powder and surface.

A significantly higher flurbiprofen transport was measured over 4h from the Mini B-191 FB-COONa microparticles F3 compared to F2 (4.0 ± 0.2 mg cm^{-2}, 56 ± 6% of the loading; $P < 0.05$) (Fig. 5). This result was assigned to the higher aqueous solubility (15 mg/ml in PBS pH 7.4 at 37 °C) and dissolution rate of the sodium salt of the drug. The amount of flurbiprofen recovered from the mucosa at the end of the experiment was 0.36 ± 0.02 mg for F3.

All transport profiles shown in Figure 5 were linear up to 2h of permeation and the sink conditions were verified in all cases, with the flurbiprofen concentration in the receptor solution always below 10% of the solubility in PBS pH 7.4 of the salt form. Then, the steady-state flux calculated for F3 was doubled compared to the flurbiprofen acid spray-dried microparticles F2.

The spray dryer equipment did not affect the flurbiprofen transport across the mucosa when comparing the Nano B-90 FB-COONa microparticles dried at 70 °C (F13_70) with the Mini B-191 particles (F3). In fact, their 4h transport profiles and steady-state fluxes across the mucosa were not significantly different (Fig. 5, Table 4). The mucosa contained the same amount of flurbiprofen (0.36 ± 0.03 mg). This result matched with the observed no difference in the respective *in vitro* dissolution rates (see Fig. 4).

Surprisingly, the inlet temperature of Nano B-90 spray dryer resulted to affect the drug transport, being the amount permeated per unit area significantly higher for the FB-COONa microparticles spray-dried at 40 °C (5.60 ± 0.16 mg cm^{-2} *vs* 3.61 ± 0.34 mg cm^{-2}, respectively for F13_40 and F13_70). The higher flux (Table 4) was also associated with a significantly lower amount of flurbiprofen accumulated in the mucosa (0.20 ± 0.02 mg; $P < 0.05$). The higher flux of F13_40 microparticles could derive in part from the significantly smaller size distribution of F13_40 microparticles compared to F13_70. In addition, as seen by X-ray analysis, F13_40 had a different crystallinity, characterised by the presence of a second polymorph and some amorphous content. In light of this, there is the possibility that this powder dissolved on the mucosa giving rise to the formation of a supersaturated solution. However, the respective dissolution rates on the artificial membrane were very similar for all the salt formulations. Aiming to understand the divergence between *in vitro* and *ex vivo* data, we considered again the existence of a positive combination with the mucosa, as observed

with the spray-dried flurbiprofen particles F2. With the mucosa a supersaturated solution was more likely to form because the only available solvent was the 100 µl of PBS introduced with the formulation. Conversely, the artificial membrane may have allowed extra solvent to be available from the receptor due to an osmotic effect.

Finally, the lecithin presence in the composition of the Nano B-90 FB-COONa microparticles (F15_70) did not significantly modify drug permeation compared to the composition without lecithin sprayed at the same inlet temperature (F13_70) (3.22 ± 0.41 mg cm^{-2}; $P > 0.05$). Thus, lecithin effect on *ex vivo* flurbiprofen permeation across rabbit nasal mucosa was substantially neutral, likely because flurbiprofen from the sodium salt compositions permeated extensively by itself.

4. Conclusions

The flurbiprofen spray-dried powders, in particular the ones made by the flurbiprofen sodium salt, exhibited physico-chemical and biopharmaceutical characteristics fitting the product target profile for nasal administration in view of nose-to-brain targeting. By spray drying sodium flurbiprofen microparticles, the powders dissolved at high rate and sustained the *ex vivo* drug transport across rabbit nasal mucosa for a convenient time. The manufacturing of these drug microparticles was more efficient using the Nano B-90 spray dryer not only for the yield of production. In fact, compared to the conventional Mini B-191 spray dryer, we discovered that the Nano B-90 provided particle size and crystallinity properties leading to a more suitable biopharmaceutical profile with respect to the intended nasal application. Finally, the particle resulted stable in terms of drug content and dissolution rate for the nasal product preparation. The administration technique of these powders and the *in vivo* study for flurbiprofen transport to brain will be the object of a successive study.

Acknowledgements

The Authors are grateful to prof. Valerio Bertolasi and Dr. Gabriele Bertocchi (University of Ferrara) for their valuable contribution to the X-ray analyses.

Disclosure statement

The authors report no conflict of interest.

References

[1] Hebert LE, Weuve J, Scherr PA, et al. Alzheimer disease in the United States (2010–2050) estimated using the 2010 census. Neurology. 2013;80(19):1778-1783.

[2] Prince M, Comas-Herrera A, Knapp M, et al. World Alzheimer Report 2016 - Improving healthcare for people living with dementia. London (UK): Alzheimer's Disease International (ADI); 2016. (Available from: https://www.alz.co.uk/research/world-report-2016)

[3] Pimplikar SW. Neuroinflammation in Alzheimer's disease: from pathogenesis to a therapeutic target. J Clin Immunol. 2014;34 Suppl 1:S64-69.

[4] McGeer PL, Guo JP, Lee M, et al. Alzheimer's Disease Can Be Spared by Nonsteroidal Anti-Inflammatory Drugs. J Alzheimers Dis. 2018;62(3):1219-1222.

[5] Benedict C, Grillo CA. Insulin Resistance as a Therapeutic Target in the Treatment of Alzheimer's Disease: A State-of-the-Art Review. Front Neurosci. 2018;12:215.

[6] Rubio-Perez JM, Morillas-Ruiz JM. A review: inflammatory process in Alzheimer's disease, role of cytokines. ScientificWorldJournal. 2012;2012:756357.

[7] Zhang C, Wang Y, Wang D, et al. NSAID Exposure and Risk of Alzheimer's Disease: An Updated Meta-Analysis From Cohort Studies. Front Aging Neurosci. 2018;10:83.

[8] Miguel-Álvarez M, Santos-Lozano A, Sanchis-Gomar F, et al. Non-steroidal anti-inflammatory drugs as a treatment for Alzheimer's disease: a systematic review and meta-analysis of treatment effect. Drugs Aging. 2015;32(2):139-147.

[9] Gupta PP, Pandey RD, Jha D, et al. Role of traditional nonsteroidal anti-inflammatory drugs in Alzheimer's disease: a meta-analysis of randomized clinical trials. Am J Alzheimers Dis Other Demen. 2015;30(2):178-182.

[10] Cuello AC. Early and Late CNS Inflammation in Alzheimer's Disease: Two Extremes of a Continuum? Trends Pharmacol Sci. 2017;38(11):956-966.

[11] Heneka MT, Carson MJ, El Khoury J, et al. Neuroinflammation in Alzheimer's disease. Lancet Neurol. 2015;14(4):388-405.

[12] Aisen PS. Tarenflurbil: a shot on goal. Lancet Neurol. 2008;7(6):468-469.

[13] Eriksen JL, Sagi SA, Smith TE, et al. NSAIDs and enantiomers of flurbiprofen target γ-secretase and lower Aβ42 in vivo. J Clin Invest. 2003;112(3):440-449.

[14] Meister S, Zlatev I, Stab J, et al. Nanoparticulate flurbiprofen reduces amyloid-β 42 generation in an in vitro blood–brain barrier model. Alzheimers Res Ther. 2013;5(6):51.

[15] Lehrer S. Nasal NSAIDs for Alzheimer's disease. Am J Alzheimers Dis Other Demen. 2014;29(5):401-403.

[16] Wilcock GK, Black SE, Hendrix SB, et al. Efficacy and safety of tarenflurbil in mild to moderate Alzheimer's disease: a randomised phase II trial. Lancet Neurol. 2008;7(6):483-493.
[17] Imbimbo BP. Why did tarenflurbil fail in Alzheimer's disease?. J Alzheimers Dis. 2009;17(4):757-760.
[18] Biswas G, Kim W, Kim KT, et al. Synthesis of Ibuprofen Conjugated Molecular Transporter Capable of Enhanced Brain Penetration. J Chem. 2017;2017:4746158.
[19] Agrawal M, Saraf S, Saraf S, et al. Nose-to-brain drug delivery: An update on clinical challenges and progress towards approval of anti-Alzheimer drugs. J Control Release 2018;281:139–177.
[20] Djupesland PG, Messina JC, Mahmoud RA. The nasal approach to delivering treatment for brain diseases: an anatomic, physiologic, and delivery technology overview. Ther Deliv. 2014;5(6):709-733.
[21] Meredith ME, Salameh TS, Banks WA. Intranasal delivery of proteins and peptides in the treatment of neurodegenerative diseases. AAPS J. 2015;17(4):780-787.
[22] Tiozzo Fasiolo L, Manniello MD, Tratta E, et al. Opportunity and challenges of nasal powders: Drug formulation and delivery. Eur J Pharm Sci. 2018;113:2-17.
[23] Buttini F, Colombo P, Rossi A, et al. Particles and powders: tools of innovation for non-invasive drug administration. J Control Release. 2012;161(2):693-702.
[24] Balducci AG, Ferraro L, Bortolotti F, et al. Antidiuretic effect of desmopressin chimera agglomerates by nasal administration in rats. Int J Pharm. 2013;440(2):154-160.
[25] Colombo G, Lorenzini L, Zironi E, et al. Brain distribution of ribavirin after intranasal administration. Antiviral Res. 2011;92(3):408-414.
[26] Giuliani A, Balducci AG, Zironi E, et al. In vivo nose-to-brain delivery of the hydrophilic antiviral ribavirin by microparticle agglomerates. Drug Deliv. 2018;25(1):376-387.
[27] Colombo G, Langer R, Kohane DS. Effect of excipient composition on the biocompatibility of bupivacaine-containing microparticles at the sciatic nerve. J Biomed Mater Res A. 2004;68(4):651-659.
[28] Manniello MD, Del Gaudio P, Porta A, et al. Aerodynamic properties, solubility and in vitro antibacterial efficacy of dry powders prepared by spray drying: Clarithromycin versus its hydrochloride salt. Eur J Pharm Biopharm. 2016;104:1-6.
[29] Aquino RP, Prota L, Auriemma G, et al. Dry powder inhalers of gentamicin and leucine: formulation parameters, aerosol performance and in vitro toxicity on CuFi1 cells. Int J Pharm. 2012;426(1-2):100-107.

[30] Sansone F, Picerno P, Mencherini T, et al. Enhanced technological and permeation properties of a microencapsulated soy isoflavones extract. J Food Eng. 2013;115(3):298-305.
[31] Floroiu A, Klein M, Krämer J, et al. Towards Standardized Dissolution Techniques for In Vitro Performance Testing of Dry Powder Inhalers. Dissolut Technol. 2018;25(3).
[32] Bortolotti F, Balducci AG, Sonvico F, et al. In vitro permeation of desmopressin across rabbit nasal mucosa from liquid nasal sprays: the enhancing effect of potassium sorbate. Eur J Pharm Sci. 2009;37(1):36-42.
[33] Colombo G, Bortolotti F, Chiapponi V, et al. Nasal powders of thalidomide for local treatment of nose bleeding in persons affected by hereditary hemorrhagic telangiectasia. Int J Pharm. 2016;514(1):229-237.
[34] PubChem Compound [Internet]. Bethesda, MD (USA): National Center for Biotechnology Information, U.S. National Library of Medicine; 2018 [cited 2018 Nov 19]. Available from: https://pubchem.ncbi.nlm.nih.gov/compound/3394
[35] Belotti S, Rossi A, Colombo P, et al. Spray dried amikacin powder for inhalation in cystic fibrosis patients: a quality by design approach for product construction. Int J Pharm. 2014; 471(1-2):507-515.
[36] Belotti S, Rossi A, Colombo P, et al. Spray-dried amikacin sulphate powder for inhalation in cystic fibrosis patients: the role of ethanol in particle formation. Eur J Pharm Biopharm. 2015;93:165-172.
[37] Russo P, Sacchetti C, Pasquali I, et al. Primary microparticles and agglomerates of morphine for nasal insufflation. J Pharm Sci. 2006;95(12):2553-2561.
[38] Aquino RP, Stigliani M, Del Gaudio P, et al. Nanospray drying as a novel technique for the manufacturing of inhalable NSAID powders. ScientificWorldJournal. 2014;2014:838410.
[39] Del Gaudio P, Sansone F, Mencherini T, et al. Nanospray drying as a novel tool to improve technological properties of soy isoflavone extracts. Planta Med. 2017;83(5):426-433.
[40] Lee SH, Heng D, Ng WK, et al. Nano spray drying: a novel method for preparing protein nanoparticles for protein therapy. Int J Pharm. 2011;403(1-2):192-200.
[41] Patel BB, Patel JK, Chakraborty S, et al. Revealing facts behind spray dried solid dispersion technology used for solubility enhancement. Saudi Pharm J. 2015;23(4):352-365.
[42] Huang D. Modeling of particle formation during spray drying. Paper presented at: European Drying Conference. EuroDrying 2011; 2011 October 26-28; Palma, Baleari Island (Spain).
[43] Vehring R. Pharmaceutical Particle Engineering via Spray Drying. Pharm Res. 2008;25(5):999-1022.

[44] Santhalakshmy S, Bosco SJD, Francis S, et al. Effect of inlet temperature on physicochemical properties of spray-dried jamun fruit juice powder. Powder Technol. 2015;274: -43.
[45] Raffin R, Colombo P, Sonvico F, et al. Agglomerates containing pantoprazole microparticles: modulating the drug release. AAPS PharmSciTech. 2009;10(2):335-345.
[46] Raffin RP, Colombo P, Sonvico F, et al. Soft agglomerates of pantoprazole gastro-resistant microparticles for oral administration and intestinal release. J Drug Deliv Sci Technol. 2007;17(6):407-413.
[47] Rubino JT. Solubilities and solid state properties of the sodium salts of drugs. J Pharm Sci. 1989;78(6):485-489.
[48] David SE, Timmins P, Conway BR. Impact of the counterion on the solubility and physicochemical properties of salts of carboxylic acid drugs. Drug Dev Ind Pharm. 2012;38(1):93-103.
[49] Bottom R. The role of modulated temperature differential scanning calorimetry in the characterisation of a drug molecule exhibiting polymorphic and glass forming tendencies. Int J Pharm. 1999;192(1):47-53.
[50] Davis TD, Peck GE, Stowell JG, et al. Modeling and monitoring of polymorphic transformations during the drying phase of wet granulation. Pharm Res. 2004;21(5):860-866.
[51] Broadhead J, Edmond Rouan SK, Rhodes CT. The spray drying of pharmaceuticals. Drug Dev Ind Pharm. 1992;18(11-12):1169-1206.
[52] Illum L. Nasal drug delivery-possibilities, problems and solutions. J Control Release 2003;87(1-3):187-198.
[53] Sironi D, Rosenberg J, Bauer-Brandl A, et al. Dynamic dissolution-/permeation-testing of nano- and microparticle formulations of fenofibrate. Eur J Pharm Sci. 2017;96:20-27.

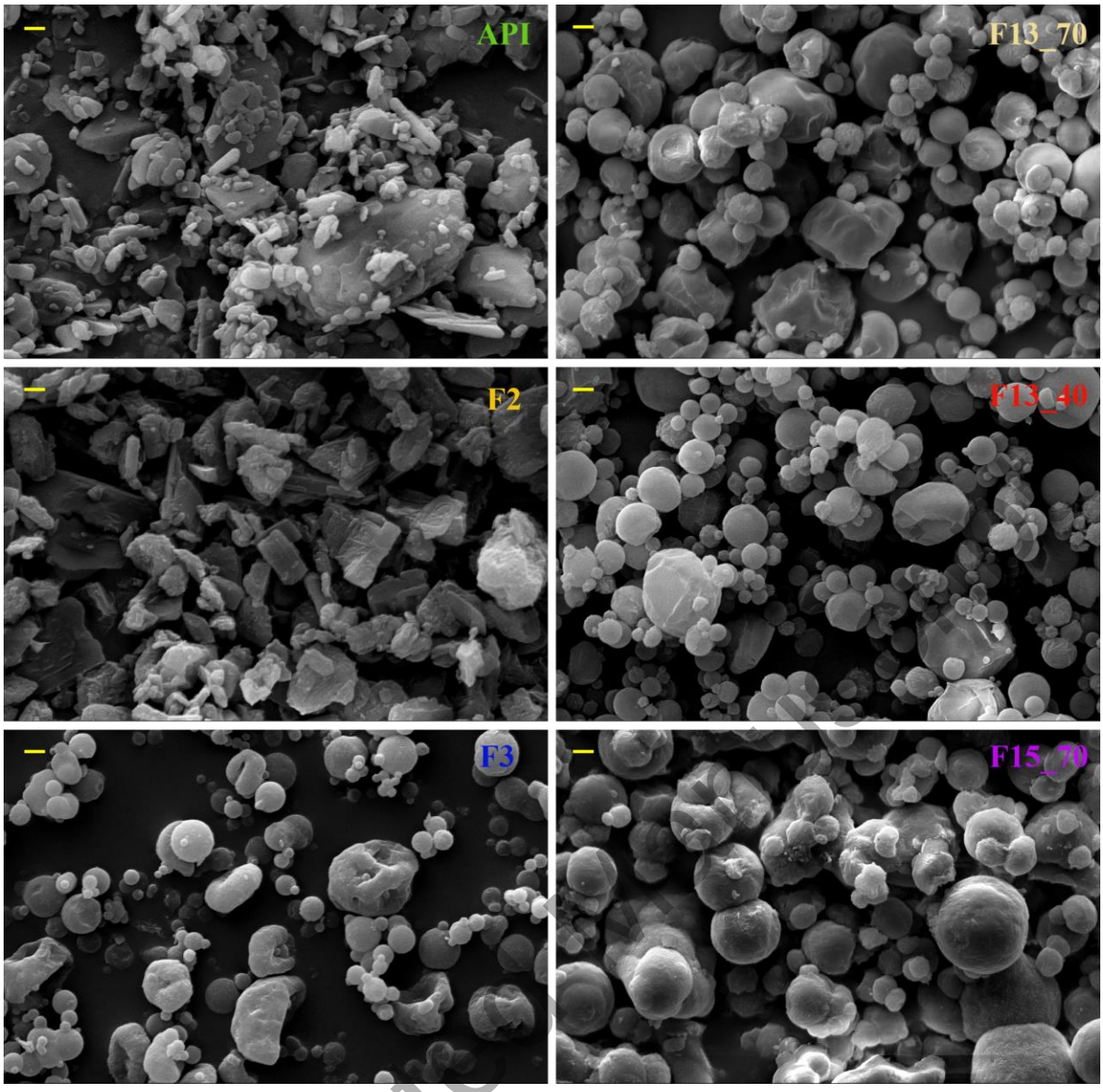

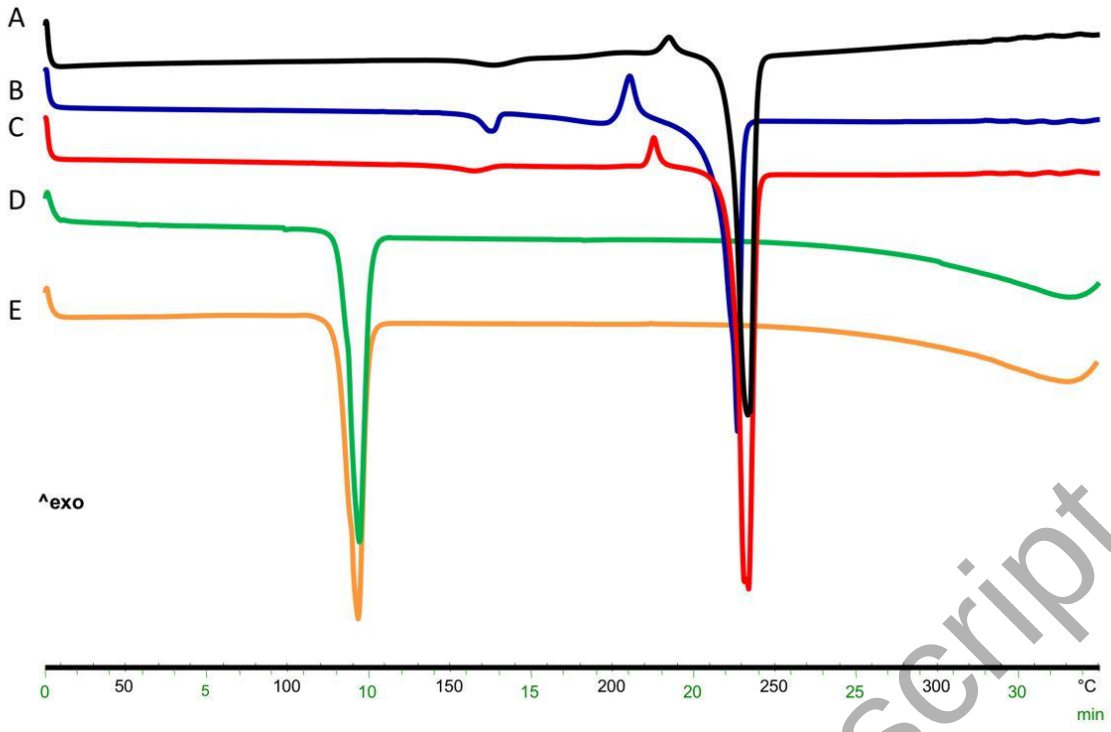

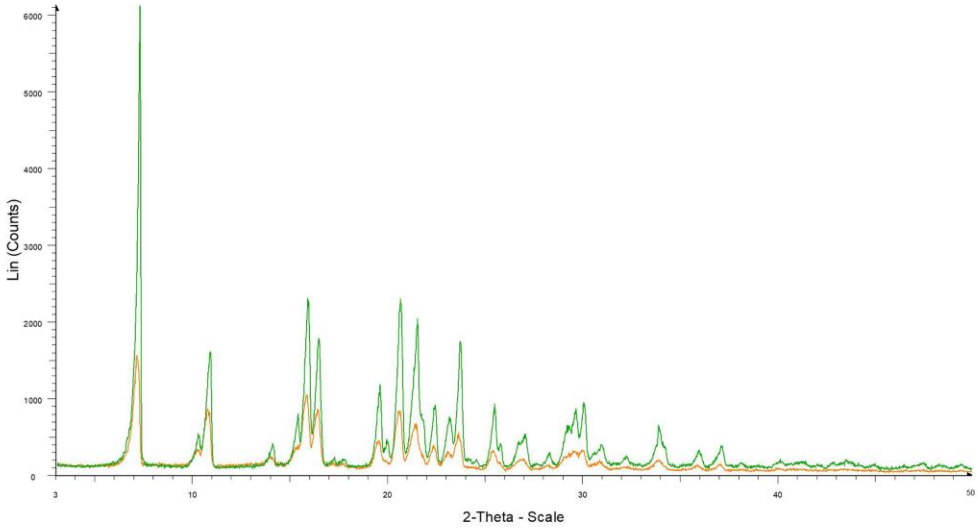

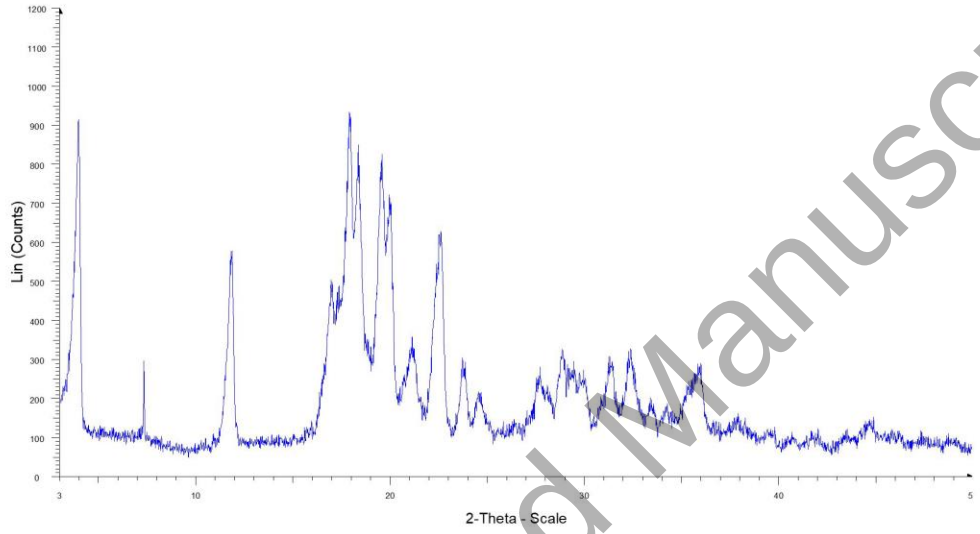

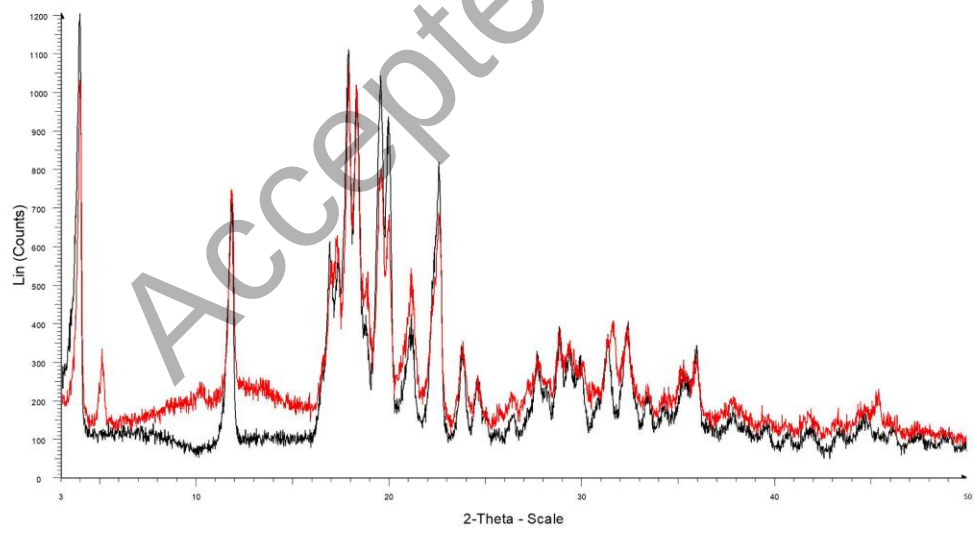

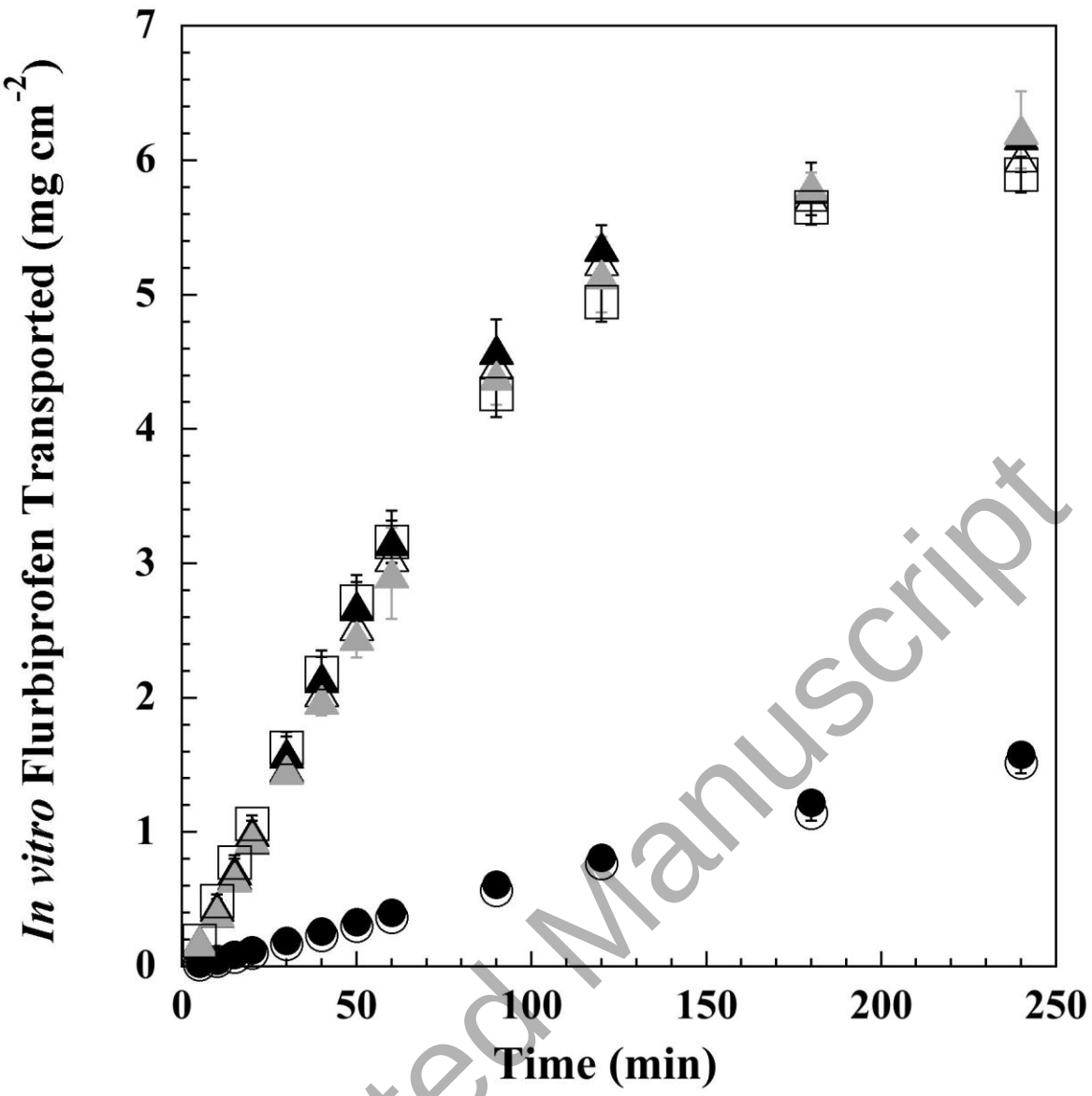

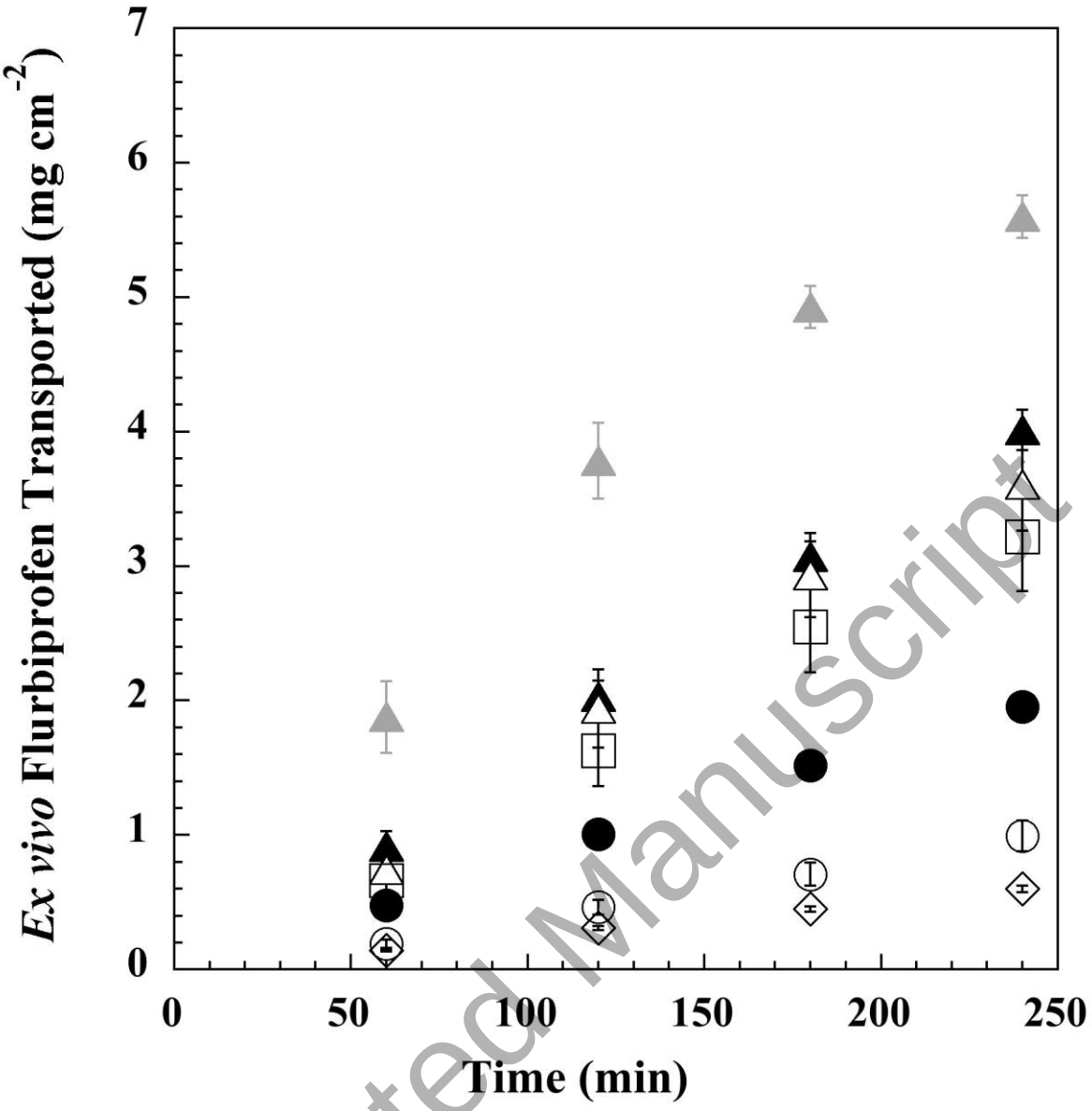

Table 1. Microparticle composition and spray drying conditions that were varied in the study (equipment type, liquid feed composition and drying temperature). Abbreviations: FB-COOH: acid flurbiprofen; FB-COONa: sodium flurbiprofen; iPrOH: isopropanol; EtOH: ethanol.

Powder Code	Spray Dryer	Liquid feed composition (% v/v)						Drying temperature (°C)	
		FB-COOH	**FB-COONa**	**Lecithin**	**H_2O**	**iPrOH**	**EtOH**	**Inlet**	**Outlet**
F2	Mini B-191	100	-	-	70	30	-	90	56-60
F3		-	100	-	100	-	-	120	65-68
F13_70	Nano B-90	-	100	-	100	-	-	70	33-34
F13_40		-	100	-	100	-	-	40	29-30
F15_70		-	92	8	95	5	-	70	30-33

Table 2. Apparatus, yield, microparticle size distribution and flurbiprofen content (mean ± standard deviation of 3 batches). One batch only of F15_70 was manufactured.

Powder	Spray Dryer	Yield (%)	Particle size (µm)			SPAN	FB-COOH content (% w/w)
			$d_{v,10}$	$d_{v,50}$	$d_{v,90}$		
Flurbiprofen raw material (API)	-		3.30 ± 0.41	16.27 ± 4.64	44.15 ± 5.09	2.58 ± 0.41	-
F2	Mini B-191	34.8 ± 1.8	4.49 ± 0.65	14.16 ± 1.51	35.43 ± 4.23	2.18 ± 0.02	99.3 ± 2.5
F3		27.3 ± 10.2	2.09 ± 0.42	10.43 ± 1.18	28.00 ± 7.06	2.46 ± 0.43	81.3 ± 0.3
F13_70	Nano B-90	76.3 ± 4.2	1.20 ± 0.10	5.69 ± 0.36	23.16 ± 7.59	3.84 ± 1.29	80.3 ± 1.8
F13_40		78.7 ± 6.4	1.62 ± 0.04	4.31 ± 0.44	10.84 ± 1.33	2.13 ± 0.08	78.7 ± 1.2
F15_70		45.6	7.42 ± 0.99	21.99 ± 1.72	49.84 ± 5.02	1.93 ± 0.11	77.1

Table 3. Temperatures and enthalpies of transition (ΔH) of Mini B-191 and Nano B-90 FB-COONa microparticles.

#	**Temperature (°C)**	**Transition**	**ΔH (J g^{-1})**
F3	163.0 ± 0.7	Endothermic event	-3.4 ± 0.2
	204.8 ± 0.6	Exothermic event	8.5±0.0
	237.7 ±0.4	Endothermic event	-63.0 ± 1.8
F13_70	164.1 ± 0.5	Endothermic event	-2.5 ± 1.6
	216.4 ± 0.8	Exothermic event	3.0 ± 0.2
	240.9 ± 0.8	Endothermic event	-74.3 ± 2.7
F13_40	157.4 ± 0.5	Endothermic event	-3.9 ± 1.5
	211.2 ± 1.3	Exothermic event	2.8 ± 0.3
	240.6 ± 0.2	Endothermic event	-85.0 ± 9.0

Table 4. Steady-state flux (J_{SS}) of flurbiprofen across regenerated cellulose membrane (mean ± SEM, n=3) and nasal mucosa (mean ± SEM, n≥5).

FORMULATION	*In vitro* Flux (μg cm^{-2} min^{-1})	*Ex vivo* Flux (μg cm^{-2} min^{-1})
Saturated solution	-	2.8 ± 0.1
Raw material	6.5 ± 0.5	4.7 ± 0.5
F2	7.0 ± 0.1	8.8 ± 0.4
F3	55.0 ± 4.0	18.6 ± 1.0
F13_70	53.2 ± 0.8	20.0 ± 2.3
F13_40	50.5 ± 5.3	31.8 ± 1.4
F15_70	54.5 ± 2.6	16.1 ± 1.8